RESEARCH ON ALGORITHMS FOR ESTIMATING KINEMATIC PARAMETERS OF A SYSTEM OF ARTICULATED RIGID BODIES BASED ON VECTORS OF ACCELERATIONS AND ANGULAR VELOCITIES OF SELECTED ONES

Bartłomiej Nalepa[1], Magdalena Pawlyta[2], Mateusz Janiak[3], Agnieszka Szczęsna[2], Konrad Wojciechowski[2,3], Aleksander Gwiazda[1]

[1] Silesian University of Technology, Faculty of Mechanical Engineering, Institute of Engineering Processes Automation and Integrated Manufacturing Systems, Konarskiego 18A, 44 – 100 Gliwice, Poland
[2] Silesian University of Technology, Faculty of Automatic Control, Electronics and Computer Science, Institute of Computer Science, Akademicka 16, 44 – 100 Gliwice, Poland
[3]Polish – Japanese Academy of Information Technology, Koszykowa 86, 02-008 Warsaw, Poland

Corresponding author: Bartłomiej Nalepa, Bartlomiej.Nalepa@polsl.pl

Abstract: Determination of kinematic parameters of articulated rigid bodies is particularly important when recreating the trajectory of movement of given systems: human (running, skiing), machines (reproducing robot motion or dedicated mechanisms). Kinematic parameters such as rotation angle between members, angular velocity and linear acceleration are determined based on measurements from IMU (Inertial Measurement Unit) sensors that are mounted on individual members. In applications, the goal is to minimize IMU elements, which e.g. can hinder human movement. In this paper, Kalman Filter estimation was used to minimize the number of IMU sensors. The model of the system was prepared on the basis of Newton-Euler equations and Denavit-Hartenberg notation. The experiments included a 3-articulated pendulum model and the following three cases: i) placing IMU sensors on all three system segments, ii) on two segments, iii) on one system segment. Removed IMU sensors were replaced by estimates based on measurements of the segment preceding the examined element. The measurement error was verified using the reference measurement with the VICON vision system.
Key words: articulated rigid bodies, accelerations and angular velocities measurement, IMU sensors, Newton-Euler equations, DH notation, numerical methods.

1. INTRODUCTION

Until now, IMU sensors (consisting of a digital gyroscope, accelerometer and magnetometer) were used to reproduce the trajectories and motion parameters of various systems of articulated rigid bodies, and the necessary analyses were performed based on the data obtained. The main application of the system is the measurement of biomechanical systems in sport or medicine. Man is put on IMU sensors in specific places, and then a measurement is made during the activity. In sport, the trajectory of the skier's movement is reconstructed [29], which allows the necessary adjustments to be made to train.

Medicine uses IMU sensors to detect a variety of pathologies in the musculoskeletal system and treatment options. IMU sensors are installed on individual links of the kinematic chain of the hand to detect possible pathologies of movement during daily vital activities [1]. Sensors are also worn on the legs to diagnose, among others ankle [2], knees [3]. Various studies have also been performed on the calibration of sensors during walking [4]. The human attitude [5] was also examined in the assessment of possible defects, to assess the correctness of the prosthesis [6], as well as to determine individual stages of gait [9, 15, 16, 22-28] as well as to estimate the size of the step [12]. The system is used to support rehabilitation for people after amputation [14].

IMU sensors are also used to analyze mechanical systems such as the pendulum [17-19,21,41,42] or the inverted pendulum [7]. Sensors are also attached to the manipulator elements for calibration [8] and for calibration of humanoid robots [10]. The system was also used to determine the mechanical parameters of an object, such as the center of mass, for a moving pendulum [11]. IMU sensors are also used to control balance maintenance in mobile robots [13]. IMU sensors are also used as elements to track human movement in real time, which allows you to control various devices [20].

Many scientific publications address the subject of IMU sensors in mechanical or biomechanical systems as diagnostic elements. The articles used various types of mathematical apparatus for processing measurement data, among others Kalman filter. However, no Kalman filter was evaluated in any work, which would estimate the results from individual IMU sensors, which would reduce the number of installed sensors and, as a result,

increase human comfort during testing.
In the first chapters of the work, a method for analyzing measurement data was developed by defining a mathematical model of articulated rigid bodies based on Denavit-Hartenberg notation. The possibility of replacing individual IMU sensors with estimated values using the Kalman filter was subsequently verified. The test results were compared with the values from IMU sensors and the test analysis was performed.

2. LAYOUT MODEL ANALYSIS

Tests on the kinematic quantities of an object consisting of articulated rigid bodies were carried out for a three-part pendulum. The measurements were made using a marker optical motion capture system (VICON) and an IMU sensor system. The vision system was used as a reference measuring device in relation to the values read and processed from the IMU sensor system. Figure 1 shows the kinematic model of the pendulum along with a description of the VICON coordinate systems and IMU sensors.

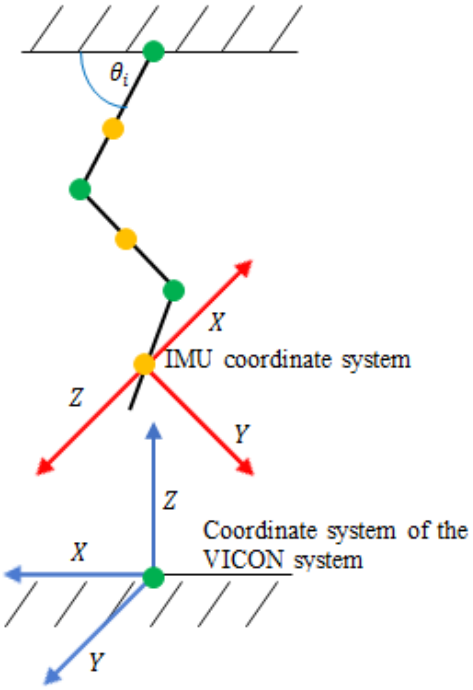

Fig. 1. The kinematic model of the pendulum along with the coordinate system of the VICON system and IMU sensors

Reconstruction of the pendulum's trajectory required determination of the value of angles between individual system members. For this purpose, Danavit-Hartenberg notation was used together with the equations of kinematics and Newton-Euler dynamics, on the basis of which the variables of the examined system were determined [30-32]:

- rotation matrix of each member together with the torsion angles of individual members (unknown values), given by equation (1):

$$ {}^{i+1}_{i}R = \begin{bmatrix} \cos\theta_i & \sin\theta_i & 0 \\ -\sin\theta_i & \cos\theta_i & 0 \\ 0 & 0 & 1 \end{bmatrix} \quad (1) $$

- position values of individual IMU sensors (known value), equation (2):

$$ {}^{i}P_{i+1} = \begin{bmatrix} P \\ 0 \\ 0 \end{bmatrix} \quad (2) $$

- angular velocity value from *i* (known value):

$$ {}^{i}\omega_i = \begin{bmatrix} W_1 \\ W_2 \\ W_3 \end{bmatrix} \quad (3) $$

- angular velocity value from *i + 1* (known value - gyro values), equation (4):

$$ {}^{i+1}\omega_{i+1} = \begin{bmatrix} G_1 \\ G_2 \\ G_3 \end{bmatrix} \quad (4) $$

- angular acceleration vector from *i* (known value - value measured with the accelerometer sensor), equation (5):

$$ {}^{i}\dot{\omega}_i = \begin{bmatrix} E_1 \\ E_2 \\ E_3 \end{bmatrix} \quad (5) $$

- equation of the linear acceleration of the term *i + 1* taking into account only the acceleration of the term *i* together with the use of the rotation matrix and the values read from the accelerometer:

$$ {}^{i+1}\dot{v}_{i+1} = \begin{bmatrix} K_1 \\ K_2 \\ K_3 \end{bmatrix} \quad (6) $$

As a result of supplementing equation (6) with the values of linear acceleration from the *i + 1* term, the relationship to the *x* component was obtained:

$$ \dot{v}_x = K_1 \cos\theta_i + K_2 \sin\theta_i - PG_2^2 - PG_3^2 \quad (7) $$

Equation (7) allows determining the torsion angles of individual pendulum members and determining the pendulum's trajectory.

3. PENDULUM MOTION TRAJECTORY

The trajectory of the three-part pendulum was determined based on measurements from IMU sensors and a reference measurement using the VICON system. The system was measured in three

configurations:

- pendulum with three members without external forcing - determining the IMU sensor torsion configuration → experiment No. 1,
- pendulum with twisted members - one-pendulum pendulum with external forcing applied → experiment No. 2,
- three-pendulum pendulum with external forcing applied → experiment No. 3,
- pendulum with twisted members at a certain angle - single-section pendulum with extortion → experiment No. 4.

Figure 2 shows the first configuration of the pendulum under test and the values of torsion angles between individual members in Figures 3, 4 and 5 together with a comparison of values from the IMU sensor system and the VICON system measurement. The values of angular velocity and linear acceleration were read from IMU sensors, from which the angles of rotation of individual members were determined using DH notation. The VICON system read markers positions in the XYZ axes relative to the center of the global system.

Fig. 2. The first configuration of the pendulum

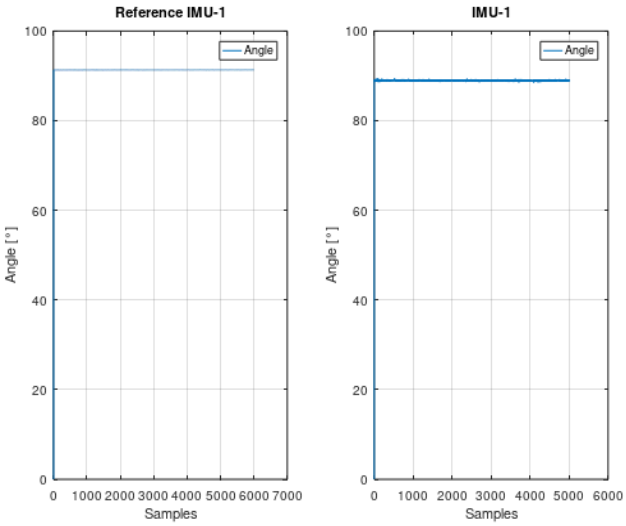

Fig. 3. Measurement of the first term - experiment1

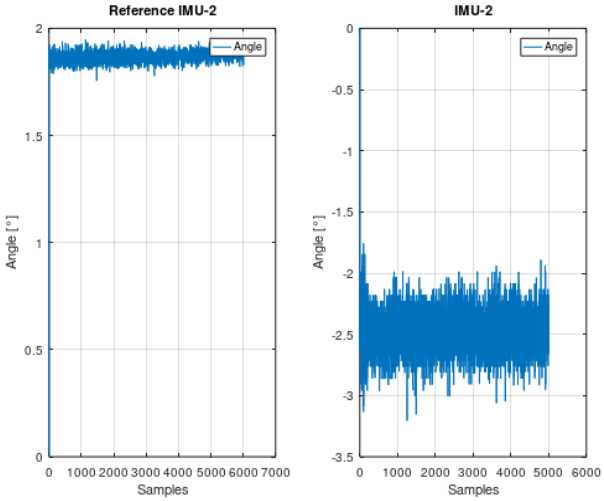

Fig. 4. Measurement of the second term - experiment 1

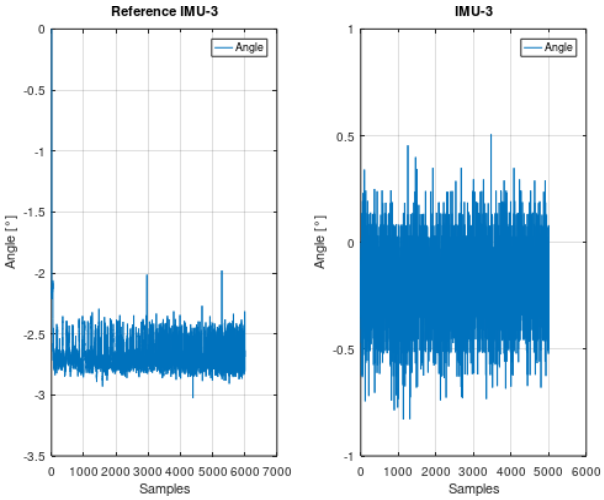

Fig. 5. Measurement of the third term - experiment 1

Measurements of the first configuration of the pendulum showed the presence of measurement noise, however, the error value of the IMU sensors does not exceed 5 degrees.

Figure 6 presents the third configuration of the pendulum and the values of the angles measured by two measuring systems (Figures. 7, 8 and 9).

Fig. 6. Second pendulum configuration

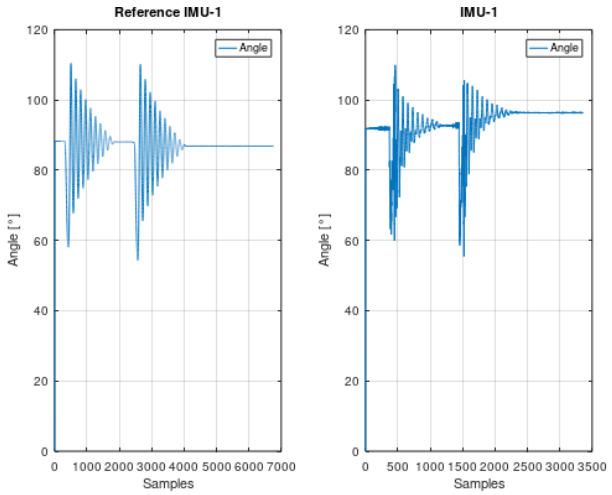

Fig. 7. Measurement of the first term - experiment 2

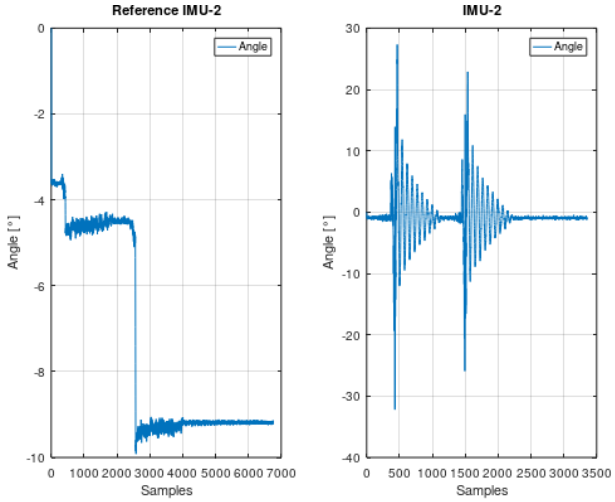

Fig. 8. Measurement of the second term - experiment 2

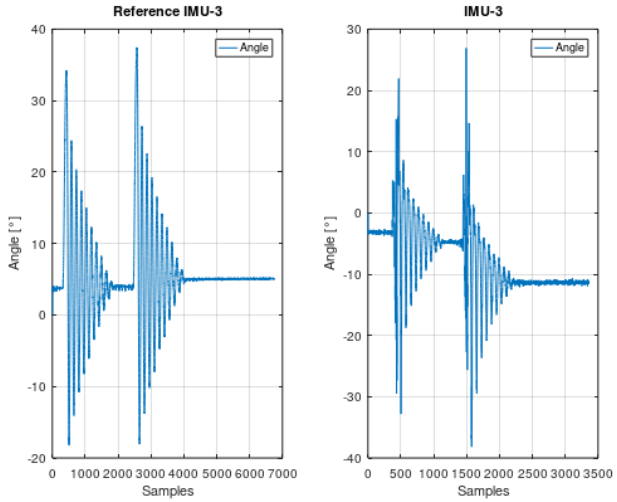

Fig. 9. Measurement of the third term - experiment 2

The measurement error when testing the second configuration increased, but the maximum error does not exceed 10 degrees.

Figure 10 presents the third pendulum configuration and trajectory graphs of two measurements (Figures 11, 12 and 13).

Fig. 10. Third pendulum configuration

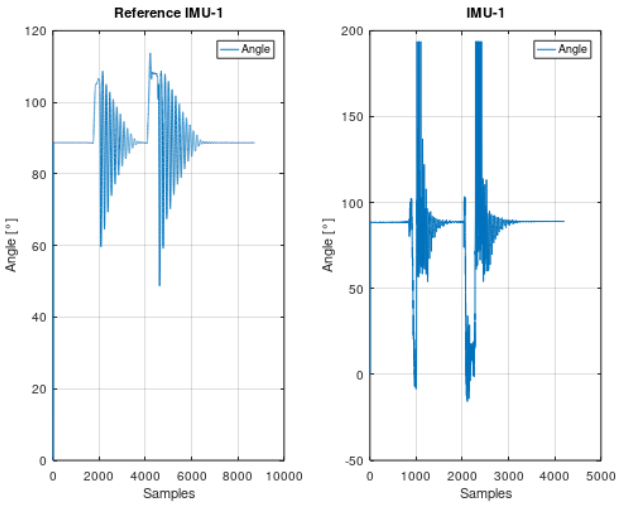

Fig. 11. Measurement of the first term - experiment 3

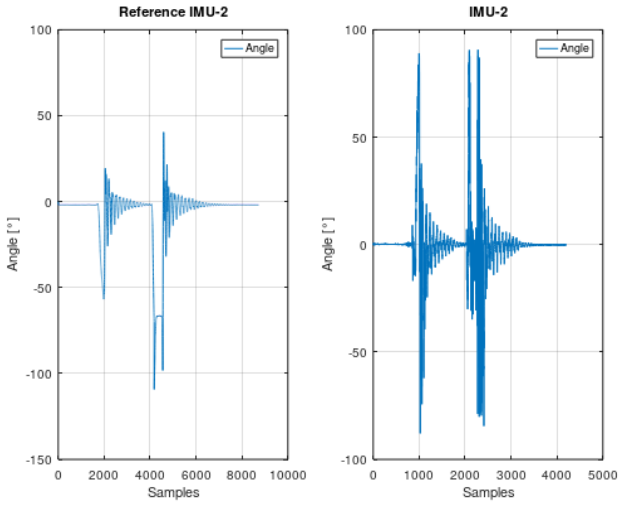

Fig. 12. Measurement of the second term - experiment 3

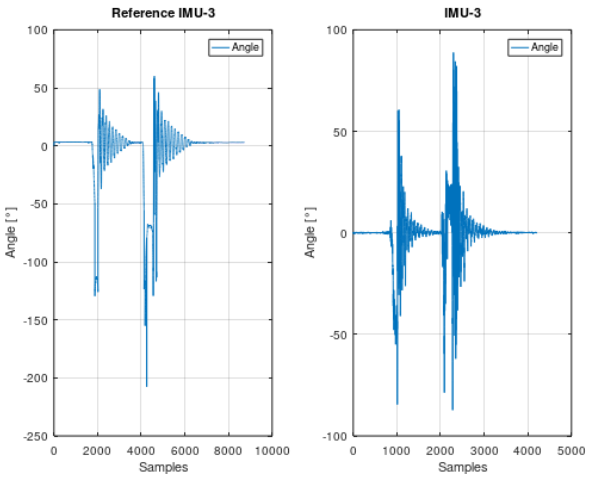

Fig. 13. Measurement of the third term - experiment3

In the third measurement, the amount of measurement noise increases, but the measurement values are similar to the reference measurement. Measurement noises may result from the values of parameters read from IMU sensors and system vibrations during initial forcing.

Figure 14 presents the fourth configuration of the pendulum and measurements of the torsion angles of individual system components in relation to two measurements (Figures 15, 16 and 17).


Fig. 14. Fourth pendulum configuration

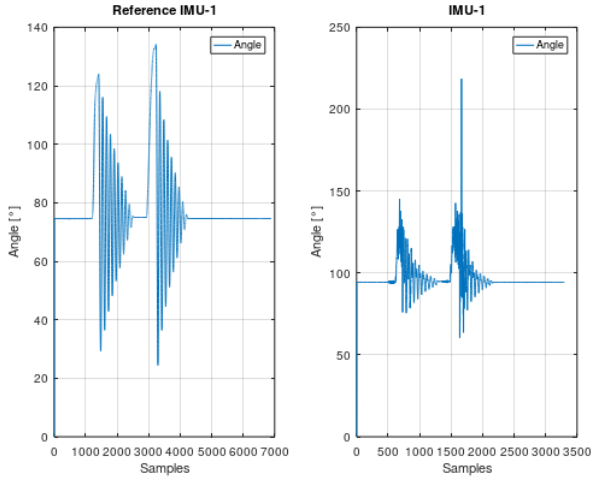

Fig. 15. Measurement of the first term - experiment 4

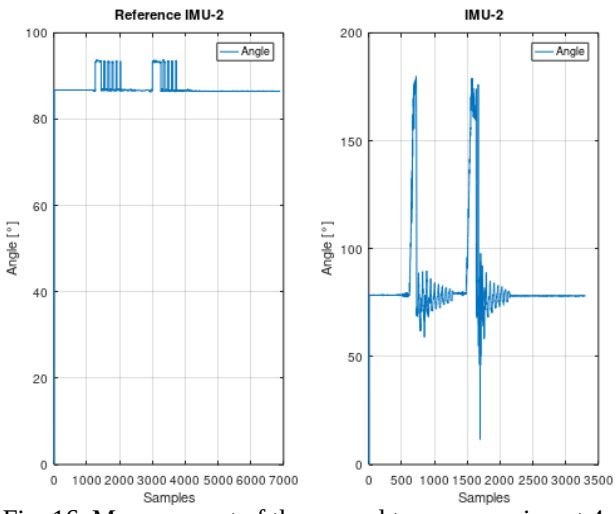

Fig. 16. Measurement of the second term - experiment 4

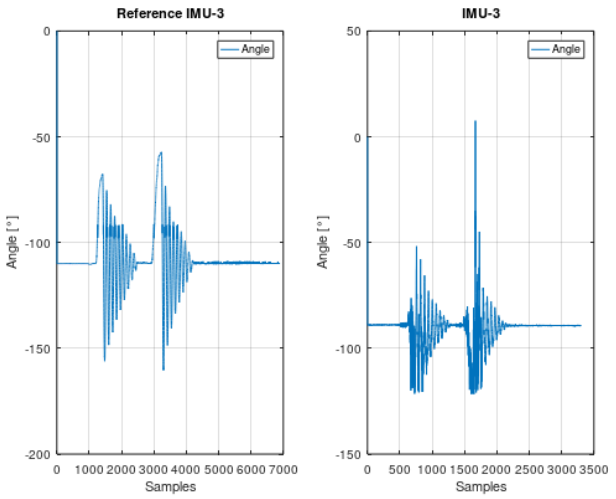

Fig. 17. Measurement of the third term - experiment 4

All measurements made with IMU sensors have a similar initial value to the reference measurement. The measurement error usually does not exceed 10 degrees. Measurement distortions result from vibrations in the system caused by initial forcing.

4. APPLICATION OF THE KALMAN FILTER

The main assumption of this article was to minimize the number of IMU sensors for use in the acquisition of human motion data. This approach will reduce the number of sensors, which will make it easier for a person to perform a given activity during measurements. It was assumed that the data from the sensors from the *i* module will allow estimating the values from the *i + 1* term. The third element of the pendulum was chosen as the element with estimated values due to the inability to clearly determine its position in space. The estimation process was carried out using the Kalman filter with a given state vector [33-36, 41]:

$$x = [\theta \quad \omega \quad \dot{\omega}]^T \tag{8}$$

The equations of circular motion obtained as a result of discretization are also written [33-36]:

$$\begin{cases} \alpha_{i+1} = \alpha_i + \lambda\omega + \frac{\lambda^2\dot{\omega}_i}{2} \\ \omega_{i+1} = \omega_i + \lambda\dot{\omega}_i \\ \dot{\omega}_{i+1} = \dot{\omega}_i \end{cases} \quad (9)$$

Measurement interference [33-36] was introduced into equation (9):

$$\alpha_{i+1} = \alpha_{i+1} + w_{\alpha i} \quad (10)$$

$$\omega_{i+1} = \omega_i + w_{\omega_i} \quad (11)$$

$$\dot{\omega}_{i+1} = \dot{\omega}_{i+1} + w_{\dot{\omega}i} \quad (12)$$

As a result of presenting equations (9 - 12) in the form, a model in the form of state equations was obtained [33-36]:

$$\begin{bmatrix} \alpha_{i+1} \\ \omega_{i+1} \\ \dot{\omega}_{i+1} \end{bmatrix} = \begin{bmatrix} 1 & \lambda & \frac{\lambda^2}{2} \\ 0 & 1 & \lambda \\ 0 & 0 & 1 \end{bmatrix} \begin{bmatrix} \alpha_i \\ \omega_i \\ \dot{\omega}_i \end{bmatrix} + \begin{bmatrix} 1 & \lambda & \frac{\lambda^2}{2} \\ 0 & 1 & \lambda \\ 0 & 0 & 1 \end{bmatrix} \begin{bmatrix} w_{\alpha i} \\ w_{\omega i} \\ w_{\dot{\omega} i} \end{bmatrix} \quad (13)$$

Output equations [33-36]:

$$\begin{bmatrix} \dot{v}_{i+1} \\ \dot{\omega}_{i+1} \\ \omega_{i+1} \end{bmatrix} = \begin{bmatrix} 1 & 0 & 0 \\ 0 & 1 & 0 \\ 0 & 0 & 1 \end{bmatrix} \begin{bmatrix} \alpha_i \\ \omega_i \\ \dot{\omega}_i \end{bmatrix} + \begin{bmatrix} w_{\alpha i} \\ w_{\omega i} \\ w_{\dot{\omega} i} \end{bmatrix} \quad (14)$$

IMU sensors allow measurement of angular velocity and linear acceleration. Figures 18, 19, 20 and 21 present graphs of measurable and estimated values for the third segment, for individual pendulum configurations.

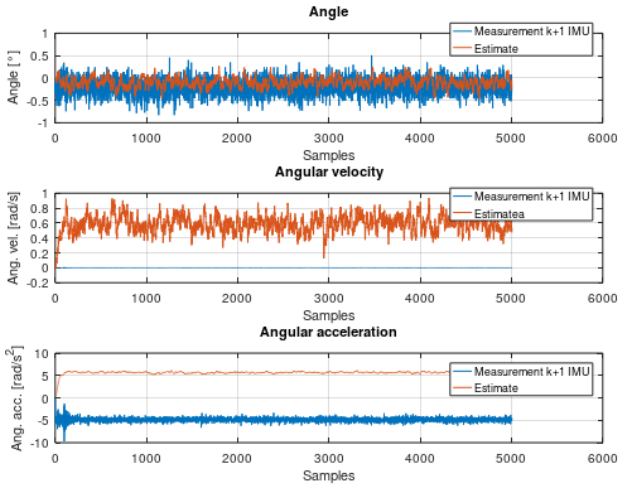

Fig. 18. First configuration of the pendulum - IMU data with estimates

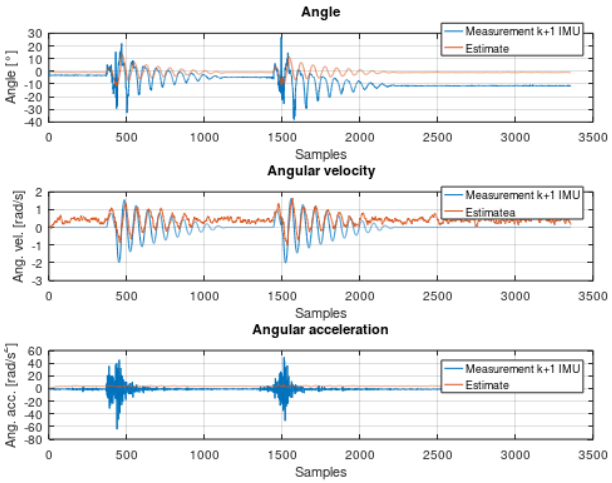

Fig. 19. Second pendulum configuration - IMU data with estimates

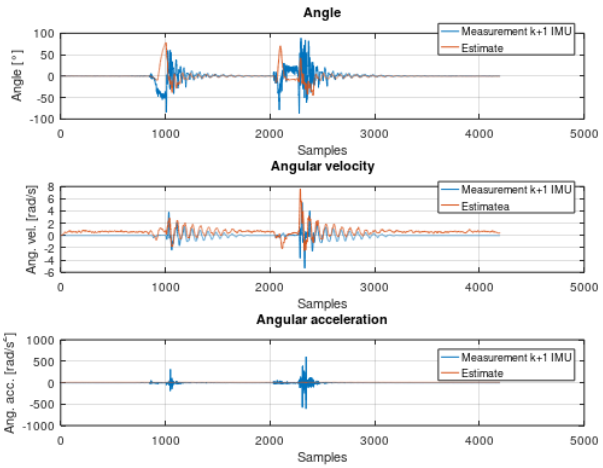

Fig. 20. Third pendulum configuration - IMU data with estimates

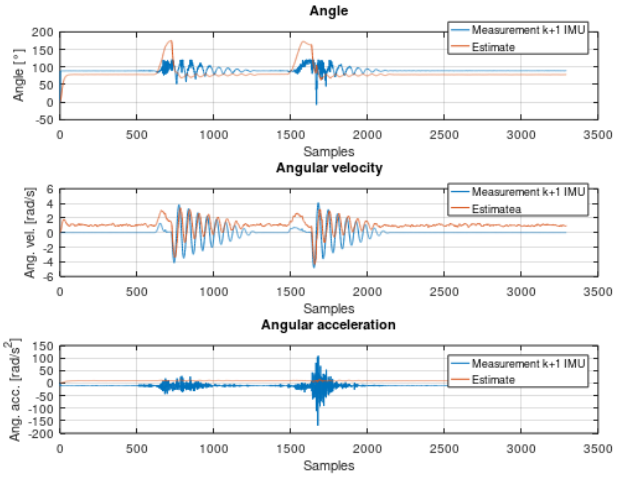

Fig. 21. Fourth pendulum configuration - IMU data with estimates

The results most similar to measurements from IMU sensors are an estimate of angular velocity. This is due to the fact that the angular velocity measurement was read directly from the IMU sensors and does not contain approximation errors resulting from mathematical operations performed on other quantities.

5. RESULTS ANALYSIS

Chapter 4 estimates the values of the third member of the pendulum. The obtained estimates were compared to the values from IMU sensors based on the DTW algorithm (Dynamic Time Warping) [37-40,43], which determined the average error between the measurement and estimated graph. The results are presented according to the pendulum configuration in Figures 22, 23, 24 and 25, for the values of angular velocities, for fragments of 800 samples - the moment of forcing.

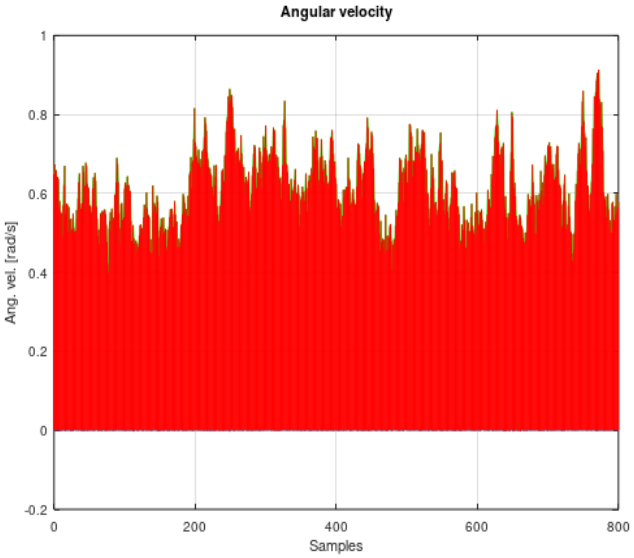

Fig. 22. The first configuration of the pendulum - DTW algorithm

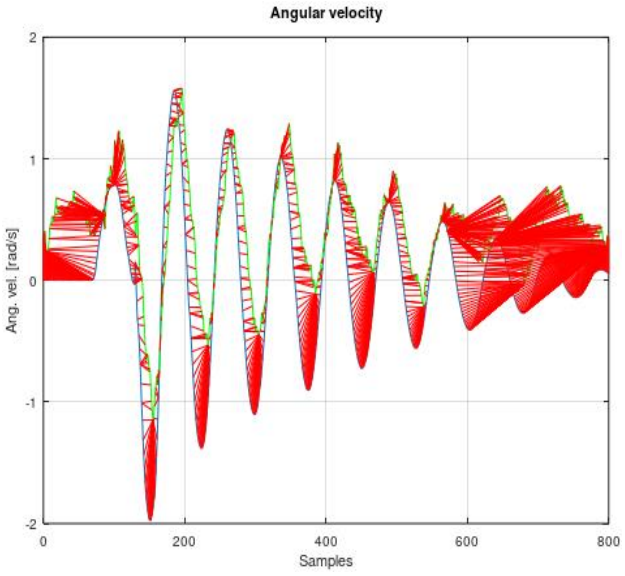

Fig. 23. Second pendulum configuration - DTW algorithm (blue graph - measured value, green graph - estimate, red lines - distance between individual points)

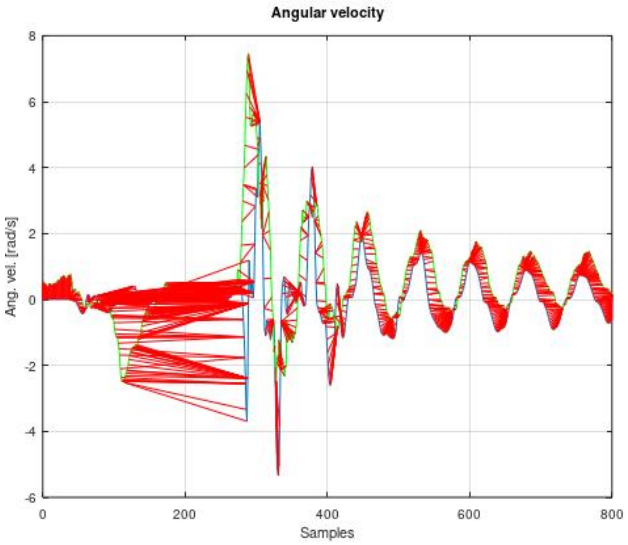

Fig. 24. Third pendulum configuration - DTW algorithm

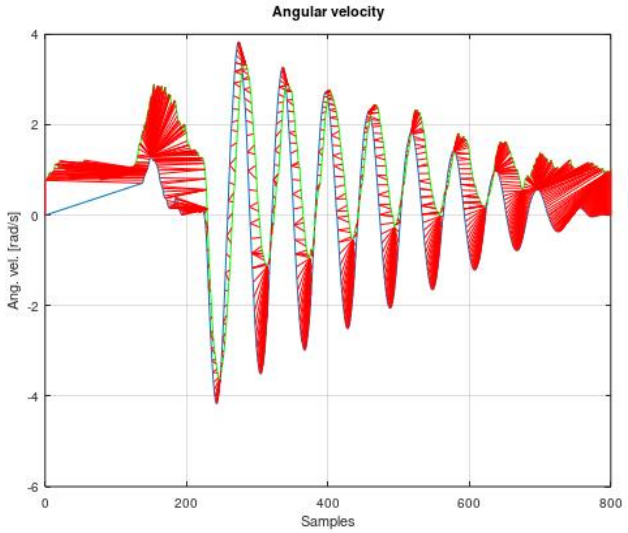

Fig. 25. Fourth configuration of the pendulum - DTW algorithm

Values of average distances between the angular velocity graph from the IMU sensor and the estimated value:

- first pendulum configuration– 0.388 $\left[\frac{rad}{s}\right]$,
- second pendulum configuration– 0.064 $\left[\frac{rad}{s}\right]$,
- third pendulum configuration–0.14 $\left[\frac{rad}{s}\right]$,
- fourth pendulum configuration– 0.457 $\left[\frac{rad}{s}\right]$.

It can be concluded from the application of the DTW algorithm that the value of the average error between the measurement of angular velocity from the IMU sensor and the estimate does not exceed0.5 $\left[\frac{rad}{s}\right]$. Taking into account the maximum and minimum values of angular velocity measurements, the error is about 25%. In the experiment, however, no algorithm was used to filter the values obtained from IMU sensors.

6. CONCLUSIONS

This article explores the possibility of minimizing the number of IMU sensors mounted on members of articulated rigid bodies. An algorithm was developed using Denavit-Hartenberg notation to determine the trajectory of motion of individual system members based on data from IMU sensors. Then, the Kalman Filter model was determined and the estimates of the measurement data were determined. The mean distance was determined based on the DTW algorithm between the angular velocity value from the IMU sensor and the estimated value.

The application of the Kalman filter gave the best results when estimating angular velocity values, which is caused by estimating the value directly from the IMU sensor without subsequent mathematical transformations. The results of angular velocities from the IMU sensor and estimated were tested with the DTW algorithm. Based on the DTW algorithm, the average distance between two graphs was determined, which allowed to determine the average error. The largest error was recorded for the first and last configuration of the pendulum. In the first configuration, the pendulum had no twisted members and no external load was applied, so the error is caused by the sensor's measuring accuracy and the lack of signal filtering. Maximum error of approx. $0.5\left[\frac{rad}{s}\right]$, constitutes about 25% error for the peak value of the pendulum measurement in the fourth configuration. The measurement error is significant, which necessitates the use of a suitable filter for measurements and artificial intelligence algorithms to correct the estimated values.

7. REFERENCES

1. Luinge, H. J., Veltink, P. H., Baten, C. T. M., (2007). *Ambulatory measurement of arm orientation*, Journal of Biomechanics, **40**, pp. 78-85.

2. O'Donovan, K. J., Kamnik, R., O'Keeffe, D. T., Lyons, G. M., (2007). *An intertial and magnetic sensor based technique for joint angle measuremen*t, Journal of Biomechanics, **40**, pp. 2604-2611.

3. Favre, J., Aissaoui, R., Jolles, B. M., de Guise, J. A., Aminian, K., (2009). *Functional calibration procedure for 3D knee joint angle description using inertial sensors*, Journal of Biomechanics, **40**, pp. 2330-2335.

4. Palermo, E., Rossi, S., Marini, F., Patane, F., Cappa, P., (2014). *Experimental evaluation of accuracy and repeatability of a novel body-to-sensor calibration procedure for inertial sensor-based gait analysis*, Measurement, **52**, pp. 145-155.

5. Picerno, P., Cereatti, A., Cappozzo, A., (2008). *Joint kinematics estimate using wearable inertial and magnetic sensing modules*, Gait & Posture, **28**, pp. 588-595.

6. Brennan, A., Zhang, J., Deluzio, K., Li, Q., (2011). *Quantification of inertial sensor-based 3D joint angle measurement accuracy using an instrumentedgimbals*, Gait & Posture, **34**, pp. 320-323.

7. Gajamohan, M., Muehlebach, M., Widmer, T., D'Andrea, R., (2013). *The Cubli: A Reaction Wheel Based 3D Inverted Pendulum*, European Control Conference (ECC), Zurich.

8. Du, G., Zhang, P., (2013). *IMU-Based Online Kinematic Calibration of Robot Manipulator*, The Scientific World Journal, ID 139738.

9. Sabatini, A. M., Martelloni, Ch., Scapellato, S., Cavallo, F., (2005). *Assessment of Walking Features From Foot Inertial Sensing*, IEEE Transactions on Biomedical Engineering, **52**, pp. 486-494.

10. Kim, S., Hong, S., Kim, D., (2009). *A Walking Motion Imitation Framework of a Humanoid Robot by Human Walking Recognition from IMU Motion Data*, 9th IEEE-RAS International Conference on Humanoid Robots, Paris.

11. Linder, J., Enqvist, M., Gustafsson, F., (2014). *A Closed-loop Instrumental Variable Approach to Mass and Centre of Mass Estimation Using IMU Data*, 63rd IEEE Conference on Decision and Control, Los Angeles, pp. 283-289.

12. Do, T., Liu, R., Yuen, Ch., Zhang, M., Tan, U., (2016). *Personal Dead Reckoning Using IMU Mounted on Upper Torso and Inverted Pendulum Model*, IEEE Sensors Journal, **16**, pp. 7600-7608.

13. Angelosanto, G., (2008). *Kalman Filtering of IMU Sensor for Robot Balance Control*, The Departament of Mechanical Engineering in partial Fulfillment of the Requirements for the Degree of Bachelor of Science in Mechanical Engineering at the Massachusetts Institute of Technology.

14. Cutti, A. G., Ferrari, P. G., Raggi, M., Cappello, A., Ferrari A., (2010). *'Outwalk': a protocol for clinical gait analysis based on inertial and magnetic sensors*, Med BiolEngComput, **48**, pp. 17-25.

15. Ferrari, A., Cutti, A. G., Garofalo, P., Raggi, M., Heijboer, M., Capello, A., Davalli, A., (2010). *First in vivo assessment of "Outwalk": a novel protocol for clinical gait analysis based on inertial and magnetic sensors*, Med BiolEngComput, **48**, pp. 1-15.

16. Fuschillo, V., (2013). *From inverted pendulum to N-link chain: inertial sensors-based assessment of movement kinematics and dynamics for functional evaluation and rehabilitation*, PhD Thesis in Bioengineering, University of Bologna.

17. Choi, K., Jang, S., (2010). *Calibration of Inertial Measurement Units Using Pendulum Motion*, Int. J. Of Aeronautical & Space Sci., **11**(3), pp. 234-239.

18. Hough, J., McGinnis, R. S., Perkins, N. C., (2013). *Benchmarking the Accuracy of Inertial*

Measurement Units for Estimating Kinetic Energy, Proceeding of the ASME 2013 International Machanical Engineering Congress and Exposition, IMECE2013-63303, California.
19. Madgwick S. O. H., Harrison A. J. L., Vaidyanathan, R., (2011). *Estimation of IMU and MARG orientation using a gradient descent algorithm*, IEEE International Conference on Rehabilitation Robotics, Zurich.
20. Miezal, M., Bleser, G., Schmitz, N., Stricker, D., (2013). *A generic approach to inertial tracking of arbitrary kinematic chains*, BODYNETS, ICTS, Boston, pp. 189-192.
21. Caroselli, A., Bagala, F., Cappello, A., (2013). *Quasi-Real Time Estimation of Angular Kinematics Using Single-Axis Accelerometers*, Sensors, **13**, pp. 918-937.
22. Tadano, S., Takeda, R., Miyagawa, H., (2013). *Three Dimensional Gait Analysis Using Wearable Acceleration and Gyro Sensors Based on Quaternion Calculations*, Sensors, **13**, pp. 9321-9343.
23. Muro-de-la-Herran, A., Garcia-Zapirain, B., Mendez-Zorrilla, A., (2014). *Gait Analysis Methods: An Overview of Wearable and Non-Wearable Systems, Highlighting Clinical Applications*, Sensors, **14**, pp. 3362-3394.
24. Casamassima, F., Ferrari, A., Milosevic, B., Ginis, P., Farella, E., Rocchi, L., (2014). *A Wearable System for Gait Training in Subjects with Parkinson's Disease*, Sensors, **14**, pp. 6229-6246.
25. Seel, T., Raisch, J., Schauer, T., (2014). *IMU-Based Joint Angle Measurement for Gait Analysis*, Sensors, **14**, pp. 6891-6909.
26. Bergamini, E., Ligorio, G., Summa, A., Vannozzi, G., Cappozzo, A., Sabatini, A. M., (2014). *Estimating Orientation Using Magnetism and Inertial Sensors and Different Sensor Fusion Approaches: Accuracy Assessment in Manual and Locomotion Tasks*, Sensors, **14**, pp. 18625-18649.
27. Pasciuto, I., Ligorio, G., Bergamini, E., Vannozzi, G., Sabatini, A. M., Cappazzo, A., (2015). *How Angular Velocity Features and Different Gyroscope Noise Types Interact and Determine Orientation Estimation Accuracy*, Sensors, **15**, pp. 23983-24001.
28. Vargas-Valencia, L. S., Elias, A., Rocon, E., Bastos-Filho, T., Frizera, A., (2016). *An IMU-to-Body Alignment Method Applied to Human Gait Analysis*, Sensors, 16.
29. Yu, G., Jang, Y. J., Kim, J., Kim, J. H., Kim, H. Y., Kim, K., Panday, S. B., (2016). *Potential of IMU Sensors in Performance Analysis of Professional Alpine Skiers*, Sensors, **16**, p. 463.
30. Craig, J.J., (2005). *Introduction to Robotics*, Mechanics and Control, Pearson Education International, New Jersey.
31. Santos, V.J., Valero-Cuevas, F. J., (2006). *Reported anatomical variability naturally leads to multimodal distributions of Denavit-Hartenberg parameters for the human thumb*, IEEE Transactions on Biomedical Engineering, **53**, pp. 155-163.
32. Corke, P. I., (2007). *A Simple and Systematic Approach to Assigning Denavit-Hartenberg Parameters*, IEEE Transactions on Robotics, **23**, pp. 590-594.
33. Bennett, T., Jafari, R., Gans, N., (2013). *An extended kalman filter to estimate human gait parameters and walking distance*, IEEE 2013 American Control Conference, Washington.
34. Wenhardt, S., Deutsch, B., Hornegger, J., Niemann, H., Denzler, J., (2006). *An Information Theoretic Approach for Next Best View Planning in 3-D*, IEEE 18th International Conference on Pattern Recognition, Hong Kong.
35. Harvey, A. C., (1989*). Forecasting, structural time series models and the Kalman filter*, Cambridge University Press, Cambridge.
36. Available from: http://jtjt.pl/filtr-kalmana, Accessed: 14/03/2019.
37. Rabiner, L., Myers, C., (1981). *Connected digit recognition using a level-building DTW algorithm*, IEEE Transactions on Acoustics, Speech, and Signal Processing, **29**, pp. 351-363.
38. Senin, P., (2008).*Dynamic Time Warping Algorithm Review*, Information and Computer Science Department, University of Hawaii at Manoa Honolulu.
39. PiyushShanker, A., Rajagopalan, A. N., (2007). *Off-line signature verification using DTW*, Pattern Recognition Letters, **28**(12), pp. 1407-1414.
40. Available from: https://nipunbatra.github.io/blog/2014/dtw.html, Accessed: 14/03/2019.
41. Szczesna, A., Pruszowski, P., (2016). *Model-based extended quaternion Kalman filter to inertial orientation tracking of arbitrary kinematic chains*, SpringerPlus 5: 1965, https://doi.org/10.1186/s40064-016-3653-8.
42. Szczesna, A., Skurowski, P., Lach, E., Pruszowski, P., Peszor, D., Paszkuta, M.mSlupik, J., Lebek, K., Janiak, M., Polanski, A., Wojciechowski, K., (2017). *Inertial Motion Capture Costume Design Study*, Sensors, **17**(3), p. 612.
43. Skurowski, P., Pruszowski, P., Peszor, D., (2016). *Synchronization of motion sequences from different sources*, AIP Conference Proceedings 1738, 180013. https://doi.org/10.1063/1.4951960.

Received: April 15, 2019 / Accepted: December 20, 2019 / Paper available online: December 25, 2019